Cement and Concrete Research 39 (2009) 36–44

Contents lists available at ScienceDirect

Cement and Concrete Research

journal homepage: http://ees.elsevier.com/CEMCON/default.asp

Water desorption and shrinkage in mortars and cement pastes: Experimental study and poromechanical model

Thomas Rougelot [a,*], Frédéric Skoczylas [b], Nicolas Burlion [a]

[a] Laboratoire de Mécanique de Lille, UMR CNRS 8107, USTL-Polytech'Lille, Cité Scientifique, 59650 Villeneuve d'Ascq, France
[b] Laboratoire de Mécanique de Lille, UMR CNRS 8107, Ecole Centrale de Lille, Cité Scientifique, 59650 Villeneuve d'Ascq, France

ARTICLE INFO

Article history:
Received 18 June 2008
Accepted 28 October 2008

Keywords:
Water desorption curves
Cement paste
Mortar
Shrinkage
Modelling

ABSTRACT

The aim of the present research was to study moisture changes and strains induced by smooth water desorption of several cement based materials. The main advantage of this small-steps drying is to dramatically limit the structural effect within tested samples, by lowering moisture gradients and therefore cracking due to differential shrinkage. Resulting data are of importance as they allow water retention curves, porosity distribution and desiccation shrinkage to be determined versus a large range of relative humidity. Experiments were conducted on ordinary mortars and cement pastes with water-to-cement ratio of 0.5 and 0.8. The role of the cementitious matrix and of aggregates over water-related behaviour of these materials can also be studied. Finally, a simple numerical model, based on experimental poromechanical results, was proposed to predict the shrinkage when the material is submitted to drying.

1. Introduction

Durability of concrete, and generally of cement-based materials, is one of the most important topics since several years (in general see [1,2]). Many studies have been carried out to describe and reliably predict their behaviour during their lifetime. Water effects appear to have a large importance as regards durability. Investigations on drying processes are crucial, since concrete structures are generally submitted to hydric gradient. This could lead to high delayed strains, occurrence of micro or macro cracks and even to a decrease in longevity.

However, tests to link shrinkage strains to drying process are usually performed using strong hydric gradients. Induced microcracking and nonhomogeneous strains are then inevitable [3]. The main issue is not only to evaluate the behaviour of the material, but also structural effects due to nonhomogeneity in moisture content through the specimen. Only few experiments have been conducted with small steps of drying, avoiding structural interferences, notably because of the time needed to get results on representative samples (here about 1.5 year). A way to reach faster saturation equilibrium is to reduce sample dimensions. Moreover, in order to better understand mechanisms that govern shrinkage versus desaturation and to obtain a representative elementary volume, it is interesting to study materials composed of only some constituents of concrete. This experimental study is presented in the first part of the article. In addition and constituting the second part, to complete these results a poromechanical approach was conducted to determine bulk modulus and Biot's coefficient of materials. A final part of the article is then devoted to the presentation of a new simple model based on these data, to show in what extent it could predict the shrinkage of cementitious materials submitted to drying.

2. Desorption curves and desiccation shrinkage

Understanding how drying process leads to desiccation shrinkage has been extensively studied (for example see [2,4,5]). But tests which aim is to link degree of saturation and strains are usually carried out by putting samples in an oven to decrease the relative humidity in which the sample is stored [6–8]. The problem is that, due to low permeability and diffusivity of concrete or mortars, a large step in relative humidity leads to a gradient in moisture content. Determining precisely the part of material effect and of structural effect on strains becomes uneasy.

Only slow drying with small steps of relative humidity can ensure a quite homogeneous distribution of moisture through the sample, and a reliable measurement of material shrinkage due to drying. Baroghel-Bouny has used this technique in part of her research, to get water vapour desorption and adsorption isotherms, and to study drying shrinkage on thin slices (3 mm) of ordinary and high-performance cement pastes and concretes [9,10]. The technique of drying by small steps in relative humidity, which seems to be the most reliable to obtain material (and not structure) data was used in this study.

2.1. Studied materials

Tests were conducted on two types of cementitious materials and for two water-to-cement ratios (W/C): cement pastes C05 with W/C

* Corresponding author.
E-mail address: thomas.rougelot@polytech-lille.fr (T. Rougelot).

0008-8846/$ – see front matter © 2008 Elsevier Ltd. All rights reserved.
doi:10.1016/j.cemconres.2008.10.005

0.5, C08 with W/C 0.8, normalized mortars M05 with W/C 0.5 and mortars M08 with W/C 0.8. Cement used was a common Portland cement CEM II/B 32.5 R. Sand for mortars was normalized sand from Leucate (France, norm EN 196-1). It is a siliceous sand, with angular shape, a maximum diameter of 2 mm and with a main modulus of about 70 GPa. The mix proportions are given in Table 1. Cement pastes allowed the cementitious matrix behaviour of a concrete to be obtained. Mortars were studied to show how aggregates could influence the behaviour under hydric "loading" due to drying. The two water-to-cement ratios tested were chosen to be high enough to ensure that after maturation, the hydration of cement is almost complete. Therefore, excessive introduced water would mainly affect the porosity of the material, not the hydration process.

2.2. Experimental study: protocols and experiments

The technique of water desorption experiments consists, at a fixed temperature, to submit the samples to a controlled desaturation. They are placed in a climatic chamber where both temperature and relative humidity (RH) can be imposed. Once equilibrium in moisture has been reached for one step of desaturation, the RH is smoothly decreased.

The tested specimens were prismatic beams of 20*20*160 mm^3 which were small enough to quickly reach moisture equilibrium (about 2 months), and large enough to be representative of the studied material. Indeed, the maximum aggregate diameter used was 2 mm, which is one-tenth of the minimum dimension of the sample, what is assumed to be representative. According to [1], the structural effect should be avoided for such a specimen if the rate of linear decrease in relative humidity is lower than about 5.10^{-3} a day. It corresponds to a linear decrease from 100% to 0% in about 200 days. The duration seems to be achieved in the present study. However, the decrease was not linear (small steps were applied); structural effect was therefore limited, but probably not totally suppressed.

The beams were moulded (two blocks for length measurements were placed at each end) and after 24 h, demoulded and put in a lime-saturated water at 20±1 °C for 5 months, that is supposed to be a sufficient time to get a complete maturation. Indeed, the variation in mass after this period is almost null. After this cure which tries to prevent autogenous shrinkage by allowing external water to enter the specimen and to fill the pore network, the sample was considered as fully saturated. It is the 100% relative humidity point. The temperature was then maintained at 20±0.1 °C and the successive steps of relative humidity were 95±1%, 90±1%, 80±1%, 65±1%, 50±1%, 30±1%. 12% RH, which was the last step, was performed by the use of LiCl salt solution. The dry state was obtained with an oven at 90 °C until complete mass stabilization, i.e. water saturation is assumed to be almost null (supposed to correspond to a relative humidity of about 3%). All kinds of materials followed the same desaturation process, and were regularly weighed with a 0.1 g precision balance, and measured with a linear transducer (resolution was 1 µm, but accuracy was about 5 µm). The equilibrium in moisture content was supposedly obtained when the loss in weight of every beam was smaller than 0.1% a week (which took about 2 months for the step 80% to 65% RH for instance).

2.3. Results

Water vapour desorption isotherms (mass water content against relative humidity) are plotted in Fig. 1a for cement pastes and in Fig. 1b for mortars. Measurements were carried out on 2 samples for each material. They showed a tiny dispersion even if it was a little more pronounced for C08 at a high humidity range. Each mark is the measure on one sample, the curve is the average of 2 samples.

Table 1
Composition of materials (mass proportion)

Material	Sand/cement	Water/cement
C05	–	0.5
C08	–	0.8
M05	3	0.5
M08	3	0.8

Similar curve shape can be observed for mortar and cement paste with the same W/C ratio. Hence this result can be evidence that hygric behaviour and "hygrostructure" of mortar cement matrix are not strongly modified with aggregates. At RH = 12%, both mortars have the same water content, whereas for higher humidities, the curves for M05 and M08 are different. The same phenomenon occurred for cement pastes. At very low humidities, the mass water content appears to be quite independent from W/C ratio, as observed in [11].

Increasing W/C ratio has an influence on the curves, mainly for RH >12%. The mass water content decreases faster with high humidities for M08 and C08, than for M05 and C05. An inversion in this tendency appears in the step 65% to 50% RH for both mortars and cement pastes. Finally, all materials between 100% and 95% RH, except C05, have a strong decrease in their mass water content. This is very important for the cure conditions during maturation. Placing specimen in a 95% RH environment will lead to a different maturation process than in a 100% RH environment, as the part of fully saturated pores strongly change between these two states.

To better understand these observations, a repartition, called r, of porous diameter versus relative humidity can be plotted. The value of r is calculated by (Eq. (1)):

$$r\left(\mathrm{RH}^{i+1}\right) = \frac{S_w\left(\mathrm{RH}^{i}\right) - S_w\left(RH^{i+1}\right)}{\mathrm{RH}^{i} - RH^{i+1}} \tag{1}$$

where RH^i stands for the relative humidity for the i-th step of desaturation (ex: for $i=0$, $\mathrm{RH}^i=100\%$) and S_w is the saturation degree for a given RH. This curve indicates which proportion of pore volume is desaturated. However, it could be useful to link relative humidity with the pore diameter, and to compare with Mercury Intrusion Porosimetry (MIP). The porosity is assumed to be a network of cylindrical capillary tubes, the Kelvin–Laplace's law can be applied for water and allows the diameter d of the thinnest desaturated pore for a given relative humidity to be calculated (Eq. (2)):

$$d = -\frac{4\gamma \cdot M}{R \cdot T \cdot \rho \cdot \ln(RH)} \tag{2}$$

where R is the perfect gas constant, T the absolute temperature, ρ the volumic mass of water, M the molar mass of water, γ the superficial tension and d the diameter of the pore. In this study, which aim is mainly comparative, only a capillary phase is taken into consideration. A model, like B.J.H [12] where the thickness of a multilayer adsorbed water in the pores is included, could have been used but would lead to only a small variation in pore diameter, which is assumed to be negligible in this comparative approach. Therefore, Eq. (1) can be rewritten as a function of the logarithmic desaturated pore diameter d^i at the i-th step of desaturation (Eq. (3)), which allows further comparison with MIP.

$$r\left(d^{i+1}\right) = \frac{S_w\left(d^{i}\right) - S_w\left(d^{i+1}\right)}{\log\left(d^{i}\right) - \log\left(d^{i+1}\right)}. \tag{3}$$

The pore diameter at 100% RH is assumed to be 100 nm, according to MIP measurement, since there are almost no pore diameters larger than 100 nm. This pore distribution is plotted in Fig. 2.

Three main peaks of porosity can be shown, as noticed by [13]. The first one is for a pore diameter of about 40 nm (step 95–100% RH) for all materials except C05. This first peak includes macro pores. The second peak depends on W/C. Indeed, for M08 and C08, the peak appears in the step 65%–80% RH (10 nm>d>5 nm), and for M05 and C05 in the step 30%–50% RH (3 nm>d>2 nm). As a consequence, the decrease in W/C leads to a decrease in the diameter of this kind of

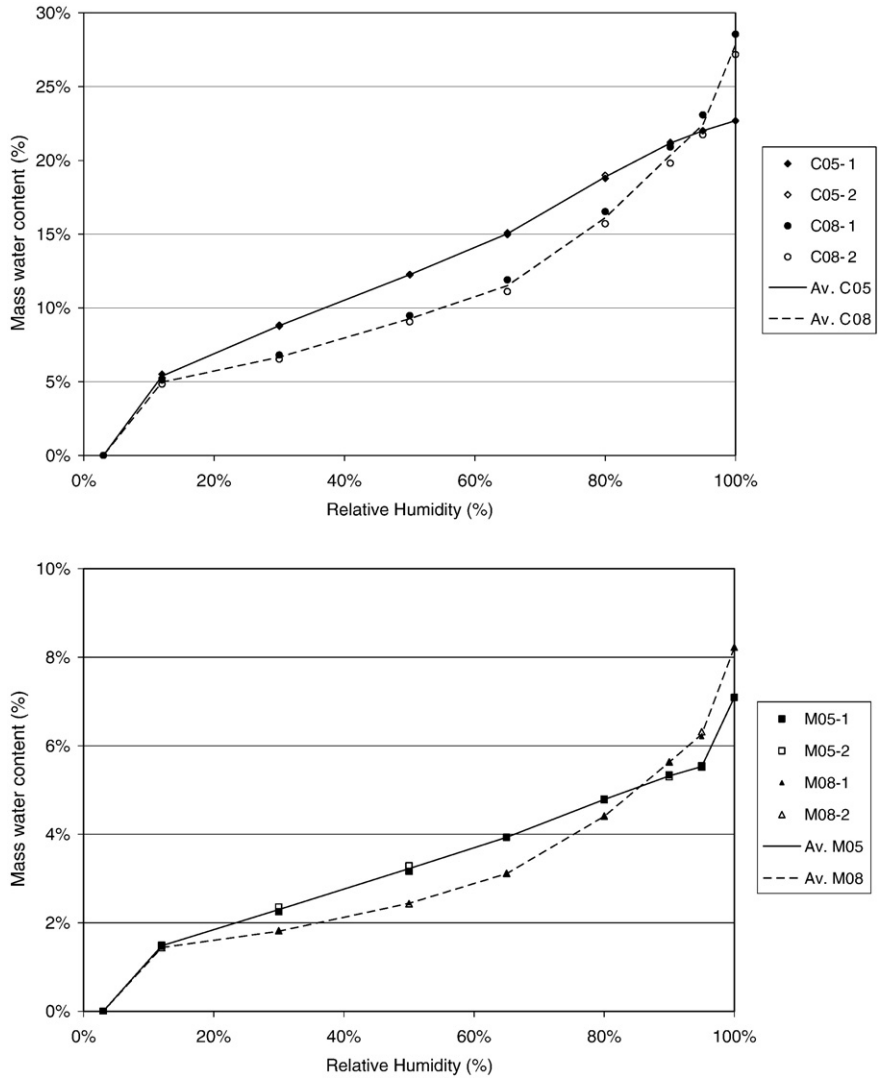

Fig. 1. Water vapour desorption curves for cement pastes (a) and mortars (b).

porosity. Finally, the last peak is in the step where specimens are dried in an oven (90 °C). It is quite equivalent for the four materials and this is a confirmation of the observations made with Fig. 1a and b for lowest humidities, as the finest porosity seems to be independent on material type. This could be explained by the fact that the structure of C–S–H will not be strongly affected by a higher water-to-cement ratio. At a given W/C, the proportion of pores and their diameters appear to be not really affected by the presence of rigid inclusions. The hygrostructure is therefore quite independent on aggregates, and the possible interfacial transition zone around inclusions seems to have no effect.

To complete this material hygrostructure study, MIP was conducted on oven-dried specimens (60 °C), despite problems that concern cement-based materials which tend to misallocate the pore size [14]. The network connectivity can have a great influence, mainly for the first peak, over measured pore diameters, which could be shifted to lower diameters due to inaccessibility of pores [13]. However, this leads to an approximate porosity distribution for pores larger than 6 nm, but remains a tool to compare the porosity of different cementitious materials. Mercury intrusion completes the distribution obtained by water desorption, especially for larger pores. The results are given in Fig. 3. The pore distribution is calculated like in Eq. (3), the saturation in water being replaced by saturation in mercury vapour. The first peak seems to match with the first peak of Fig. 2. There is apparently no difference between C05 and other materials as regards larger pores. This was not the case with the desorption method. The difference could rise from the mercury intrusion and water desorption techniques which do not act in the same way (intrusion versus desorption) and with the same interstitial fluid (mercury vapour versus water). In addition, mercury intrusion is performed with oven-dried samples. The drying process of specimen could lead to microcraking and to an increase in the pore connectivity, giving access to unreachable porosity in saturated ones.

Higher W/C ratio increases the pore diameter and is a confirmed tendency. But aggregates tend also to modify this repartition, since C05 peak is at 77 nm, and M05 peak at 62 nm. For M08 and C08, differences are stronger, since either peak value or shape of the repartition is not identical. A “pre-peak” exists on M08 curve at a diameter of 150 nm, followed by the main peak at 77 nm, but could be also explained by lack of connectivity in the pore network. On C08 curve, the unique peak is at 95 nm. For lower diameters (about 30 nm), a second “peak” could be seen, with a small difference between 05 and 08 materials. This “peak” could be linked to the second peak observed by means of water desorption on Fig. 2, even if pore sizes are different. For the lowest diameters (about 6 nm), all curves tend to have the same shape. The last peak of Fig. 2 is probably unreachable by MIP.

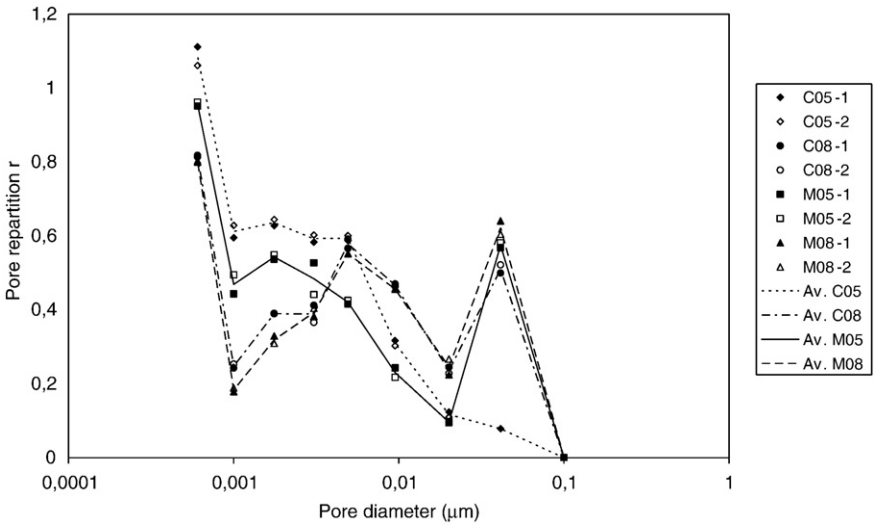

Fig. 2. Pore repartition measured by water desorption.

The total porosity was measured by two means: by drying a saturated specimen of known dimensions (cylindrical specimen, diameter 36 mm, thickness: 10 mm) at 90 °C, or by the beams used for the desorption curves. Results are given in Table 2. Even if the desorption lasted about 1.5 year, the calculated porosity is similar (except for M08) for both types of samples. This confirms that hydration of cement was achieved at the beginning of the desorption experiment, since about the same quantity of water is lost during measurement of porosity by both methods. A difference is only noticeable for M08, but explaining this phenomenon with performed experiments remains difficult. A small carbonation, essentially for materials with high W/C ratio, is experienced, but the choice of relatively "large" samples limits the perturbation due to this effect.

Such experiments were also used to measure shrinkage versus relative humidity (Fig. 4). The cementitious matrix shrinks whereas siliceous aggregates are considered as insensitive to relative humidity variation. As a consequence, a better comparison can be made if the desiccation shrinkage is normalized by cementitious matrix volume, as presented in Fig. 5. For high RH until 60%, the shrinkage appears to be globally linearly linked to relative humidity for cement pastes and mortars, which is coherent with literature observations [9]. Capillary pressure could be the mechanism leading to the observed strains [15,16]. Some authors attribute this shrinkage to variation in disjoining pressure [17], or even to both capillary and disjoining pressure [18]. Under 45% RH, capillary is not the main mechanism, and desiccation shrinkage could be attributed to variations in surface energy of C–S–H [19] and in disjoining pressure.

However, a more precise study of the shrinkage curves shows the slope of the curves gradually decreases as relative humidity decreases, whatever the tested material. As RH decreases, capillary suction increases, but there are less and less saturated pores. It can be then assumed that capillary pressure acts on a solid volume that is getting smaller. Therefore, there is probably a competition between these two opposite phenomena that can lead to a change in the slope of shrinkage. The proposed model in the next part will be based on this assumption.

Finally, the role of aggregates and of W/C ratio is also well shown on Fig. 5. Even normalized by cementitious matrix volume, mortar shrinkage, for a same W/C ratio than for cement pastes, is strongly lower. Aggregates tend to decrease by 50% for W/C=0.8 and by 52% for W/C=0.5 the

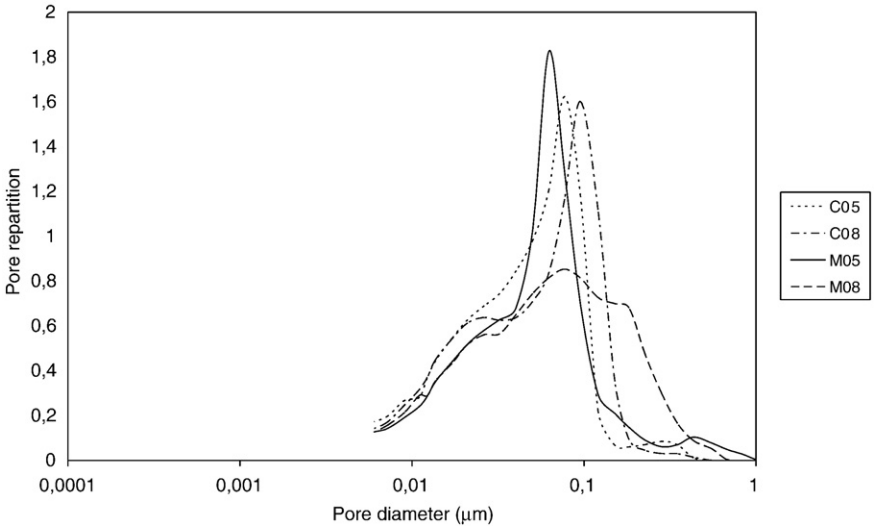

Fig. 3. Pore repartition measured by mercury intrusion.

Table 2
Porosity of materials

Material	Porosity (oven)	Porosity (desorption then oven)
	%	%
C05	38	37
C08	44	42
M05	17	16
M08	23	18

shrinkage observed for the sole cementitious matrix. In this way, the influence of rigid inclusions is quantified, avoiding structural (due to the geometry of the sample) effect during drying. A higher W/C ratio, for cement pastes and mortars, leads to an increase in desiccation shrinkage that appears to be quite evident mainly as porosity is also increased.

3. Poromechanical approach

Models predicting shrinkage in function of drying have been proposed yet [20–23], but rarely for different steps of homogeneous moisture contents in a sample. Experimental data presented in the previous part showed a great dependency of shrinkage versus relative humidity with the kind of material (cement paste, mortar) and the W/C ratio. In the objective of proposing a simple numerical model able to predict shrinkage for a given RH, a poromechanical approach could be of interest. Measuring the bulk modulus of the solid matrix (cementitious matrix, aggregates) and of the skeleton (solid matrix and connected porosity) should lead to a model that could be applied to a large extent of porous materials where capillary pressure can be considered as the main mechanism of shrinkage.

3.1. Experimental study

As capillary pressure can be considered as being a negative pore pressure at the beginning of the shrinkage, poromechanical tests were conducted on previously described materials. The specimen used for this poromechanical study was moulded cylindrical samples (diameter 36 mm length 72 mm) matured in lime-saturated water for 5 months. They were instrumented with 2 lateral and 2 longitudinal strain gauges. They were tested in a triaxial cell in which the confining pressure and the pore pressure was controlled by Gilson® pumps. The injected fluid in pores is argon in its gaseous phase. Argon pressure was applied on both sample sides which was fully water saturated. Gas pressure was then transmitted from gas to liquid which could be assumed as being pore pressure. This assumption can be made as such a test does not change water sample saturation. This allowed sound materials to be tested.

According to Biot's theory, a saturated porous material is regarded as a superposition of two continua: skeleton and pore fluid. From a thermodynamics point of view, it is an open system which exchanges fluid mass with the exterior. The state variables are the strain tensor of the skeleton (ε) and the fluid mass change per initial volume m. The associated thermodynamic forces are the total stress tensor (σ) and the pore pressure P. In fact, the pore pressure is an indirect thermodynamic force since the direct force associated with m is the enthalpy. However for experimental identification purposes, it is preferable to use pore pressure instead of enthalpy. For an elastic porous isotropic material, the state equations are for a saturated medium [24]:

$$\begin{cases} \sigma_{ij}-\sigma_{ij}^{o} = 2G_b\varepsilon_{ij} + \left(K_b - \dfrac{2G_b}{3}\right) tr(\varepsilon)\delta_{ij} - b(P-P_o)\delta_{ij} \quad \text{(a)} \\ \text{or} \\ \sigma_{ij}-\sigma_{ij}^{o} = 2G_u\varepsilon_{ij} + \left(K_u - \dfrac{2G_u}{3}\right) tr(\varepsilon)\delta_{ij} - bM\left(\dfrac{m}{\rho_o^{fl}}\right)\delta_{ij} \quad \text{(b)} \\ P-P_o = M\left(-btr(\varepsilon) + \dfrac{m}{\rho_o^{fl}}\right) \quad \text{(c)} \end{cases} \tag{4}$$

where δ_{ij} is the Kronecker symbol. σ_{ij}^{o} and P_o are initial stresses and pore pressure. Eq. (4)a and Eq. (4)b are equivalent and commonly considered as drained behaviour for Eq. (4)a or undrained behaviour for Eq. (4)b. They generalised Hooke's law for a porous material. K_b and G_b are respectively the drained bulk modulus and shear bulk modulus, b is the Biot coefficient, K_u and $G_u = G_b$ are respectively the undrained bulk modulus and shear bulk modulus, and M is the Biot modulus.

For a drained test where the interstitial pressure P_i remains constant while the confining pressure P_c is varying by ΔP_c, the volumetric strain $\Delta\varepsilon_v$ can be calculated from Eq. (4)a by Eq. (5):

$$\Delta\varepsilon_v = \frac{\Delta P_c}{K_b}. \tag{5}$$

As shown in [24], any loading step, in which the variation in confining and interstitial pressures are the same ($\Delta P_c = \Delta P_i$), leads to a volumetric strain of the sample being that of the matrix —i.e. $\Delta\varepsilon_v$

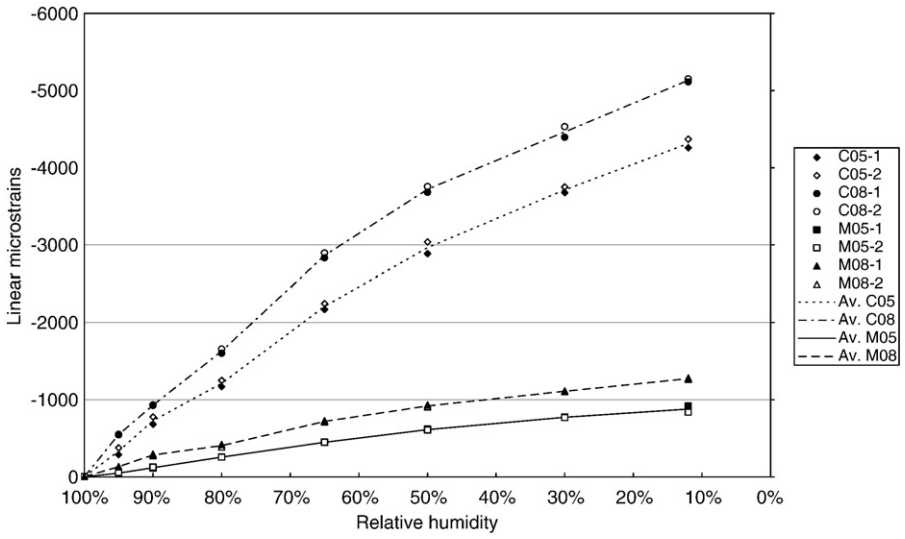

Fig. 4. Linear shrinkage versus relative humidity.

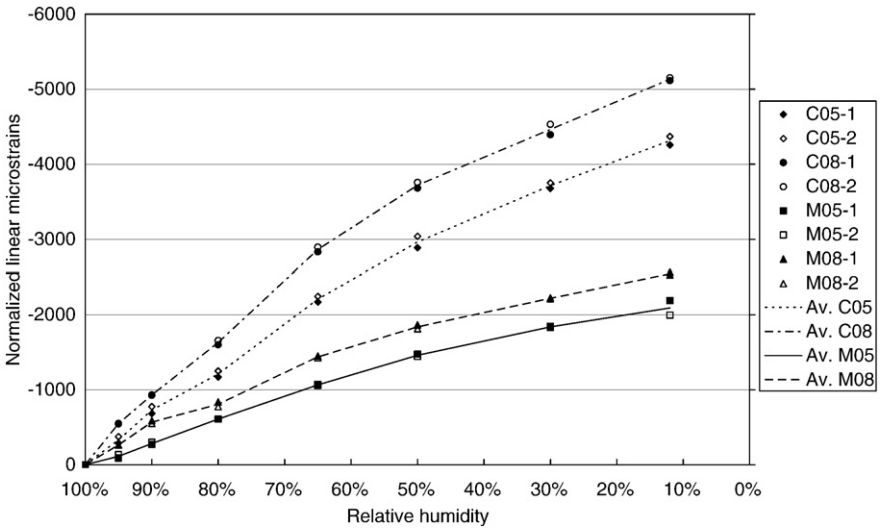

Fig. 5. Linear shrinkage versus relative humidity (volume of cementitious matrix, included porosity, is normalized).

(skeleton)=$\Delta\varepsilon_{vm}$ (matrix) whose bulk modulus K_m derives from Eq. (6) below:

$$\Delta\varepsilon_{vm} = -\frac{(\Delta P_c = \Delta P_i)}{K_m} \tag{6}$$

As a consequence, a test in which pore pressure is varied by ΔP_i while confining pressure remains constant, will lead to the modulus H to be measured with:

$$\Delta\varepsilon_v = \frac{\Delta P_i}{H}. \tag{7}$$

The modulus H has no particular name, and characterizes the volumetric strains of the material with variation in interstitial pressure. From Eqs. (5)–(7), it comes:

$$\frac{1}{K_m} = \frac{1}{K_b} - \frac{1}{H}. \tag{8}$$

Once K_m is known, Biot coefficient can be derived from:

$$b = 1 - \frac{K_b}{K_m}. \tag{9}$$

More detailed explanations on experimental measurement of poromechanical properties are given in [25]. The results for bulk modulus are given in Table 3, and for matrix modulus in Table 4. They are compared to other results obtained on same samples, but which were previously dried in an oven (90 °C) until mass equilibrium was reached. The pore network is considered as empty of water, and gas pressure is directly transmitted to the whole accessible network. The value of bulk matrix modulus is very sensitive and dispersive, and could be partly due to intrinsic variability in tested materials. Experimental set-up explains also this dispersion. The precision of K_b is about 15% on dry samples. A confirmation in the observed values could be made by submitting specimens to uniaxial compression, recording through strain gages axial and transversal strains. This would allow to obtain the Young's modulus E and Poisson's ratio ν, and a value of the bulk modulus K_b by Eq. (10)

$$K_b = \frac{E}{3(1-2\upsilon)}. \tag{10}$$

Despite this dispersion, values of K_b are coherent: a more porous (higher W/C ratio) material exhibits a lower bulk modulus, and the addition of rigid aggregates increases this value. The influence of measuring K_b on sound saturated or quickly dried specimen appears quite well in values reported in Table 3, showing a decrease in K_b for oven-dried specimen. This could be explained by microcracking due to differential shrinkage.

The K_m value is even more dispersive. Oven-dried and saturated samples have almost the same values of K_m, what remains coherent, since cracking due to quick drying will mainly affect the pore network and not the solid phase. Moreover, mortars exhibit a higher K_m than cement pastes, due to aggregates that are rigid inclusions which tend to rigidify the solid matrix. However, it is assumed that the bulk matrix modulus for a material with W/C ratio equal to 0.5 is higher than for W/C=0.8, since adding water should not increase the incompressibility of the skeleton, and even decreasing it [26]. Indeed, the "closed" porosity in the matrix probably becomes higher. However, the obtained results tend to show that this assumption is not respected. The method of measurement implies that a small variation in the measure of H or K_b could lead to a great change in the K_m value, and could explain this unexpected observation. As a partial conclusion, results remains globally conform to expected values. Yet, due to the quite large dispersion of the measured values, particular attention will be paid when used in the numerical model.

3.2. Modelling shrinkage

The basis of the proposed poromechanical model lays on some major hypotheses. Firstly, only linear elasticity is taken into consideration,

Table 3
Bulk modulus of materials

Material	Saturated sample (Mpa)	Dried sample #1 (Mpa)	Dried sample #2 (Mpa)
C05	10,500	9500	7900
C08	6400	6300	5100
M05	19,700	12,400	–
M08	12,700	10,100	8200

Table 4
Matrix modulus of materials

Material	Saturated sample (Mpa)	Dried sample (Mpa)
C05	–	24,600
C08	20,700	31,900
M05	34,100	33,400
M08	46,300	42,300

excluding eventual damage due to differential shrinkage between rigid inclusions and cementitious matrix [27], or creep. Secondly, the porous network is supposed to be constituted of cylindrical tubes equally dispersed in the sample, and that desiccation shrinkage is only due to capillary pressure variations. The model is assumed to be representative for high RH, above 50%. Moreover, each pore of a fixed diameter is in one of the two following states: saturated if the desaturated diameter calculated by Kelvin's equation (Eq. (2)) at a given RH is higher than the pore diameter, and totally desaturated otherwise. In a further study, using a more complex porous network, taking into consideration the fact that inkbottle pore geometry can exist [28]. In this first approach, which is resolutely simple, this geometry will be neglected. Finally, the last main hypothesis is to consider that capillary pressure only acts in nondesaturated pores. Indeed, when the specimen is submitted to drying from 100% RH to 95% RH, according to Eq. (2), each pore of diameter larger than about 41.5 nm is assumed free of water, whereas the rest of the pore network is submitted to a negative pressure of about 7 MPa. At each step, the percentage of the saturated pores decreases whereas the applied pressure increases. In the proposed model, the partially saturated material is considered as a saturated material in which desaturated pores are included in the matrix as "closed" porosity. This leads to a decrease in K_m when the saturation becomes lower. The bulk modulus K_b remains unchanged.

When the material is totally saturated, K_m must be equal to K_m measured in the poromechanical experiment. When totally dried, K_m becomes equal to K_b, since all pores are included in the matrix as "closed" porosity.

As a consequence, a function which describes the variation of K_m with saturation between the initial $K_m^{Sw=1}$ and K_b has to be chosen. For a first simple model approach, it is supposed linear (Eq. (11)):

$$K_m(S_w) = S_w K_m^{Sw=1} + (1-S_w)K_b. \tag{11}$$

Therefore, the Biot coefficient depends on saturation. The strains are calculated from Eq. (4)a when they are due to pore pressure only. The state's reference is a totally saturated sample ($\varepsilon_v=0$ when capillary pressure $P_{cap}=0$ MPa) and Eq. (4) can be written as:

$$\varepsilon_v = \frac{b(S_w)P_{cap}}{K_b}. \tag{12}$$

Results are given in Fig. 6a (cement pastes) and b (mortars). Due to the experimental dispersion, the values of measured K_b and K_m which best fit experimental results (called "best" values in Table 5, which are taken from Table 3 and 4), and also medium values (called "medium" values in Table 5) are used in the model. These medium values are calculated as the average of the measured K_b values, and for K_m, taking

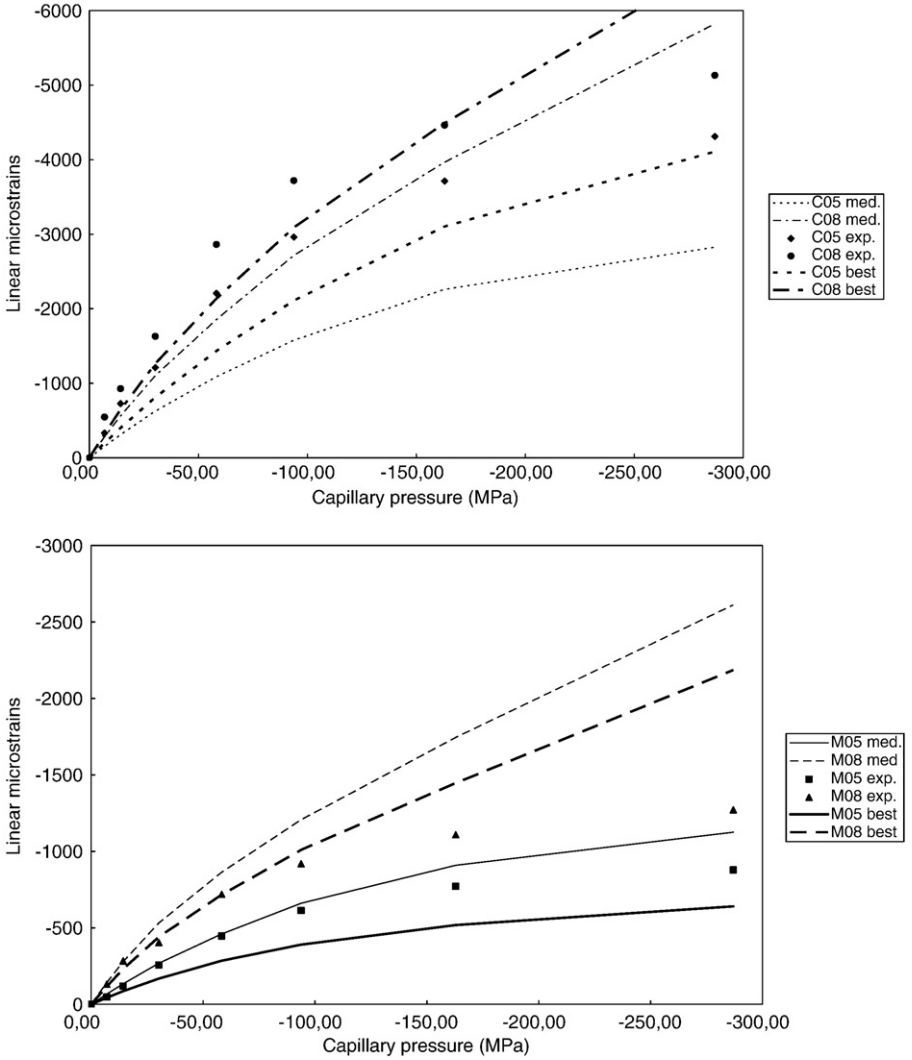

Fig. 6. a and b — Comparison between experimental and modelled linear shrinkage versus capillary pressure: "exp" stands for experimental values, "best" for best experimental values of K_b and K_m, "med" for the modelled shrinkage taking medium values for K_b and K_m.

Table 5
Modulus of materials used as "medium" and "best" values for model

Material	"Medium" values		"Best" values	
	K_b (MPa)	K_m (MPa)	K_b (MPa)	K_m (MPa)
C05	9300	24,500	7900	24,600
C08	5900	24,500	5100	20,700
M05	16,100	34,000	19,700	34,100
M08	10,400	34,000	12,700	42,300

into consideration that K_m could not be higher in 0.8 W/C ratio materials than in 0.5 ones.

Qualitatively, the proposed model seems to efficiently model the decreasing in the slope of linear shrinkage versus capillary pressure. Quantitatively, the results seem to fit quite well experimental data for mortars between 100 and 50% of relative humidity. The beginning of the slope is in agreement with experiments, mainly for high saturations. For lower humidity, capillary pressure is not the main physical phenomenon explaining shrinkage. Therefore, it appears useless to study the validity of such a model under 50% RH (equivalent to a capillary pressure of 110 MPa), as only capillary pressures are modelled, and not disjoining pressure or variation in surface energy that are predominant in this range. Moreover, the high level of stresses to which the material is submitted could lead to creep and microcracking, even if the moisture gradients are small. The behaviour of the mortar or cement paste is probably not linear elastic anymore, but visco-elasto-plastic with damage. This could explain that the model breaks down in the low HR range.

Concerning cement pastes, the numerical calculation underestimates experimental values. The slope at the beginning of the curve is also underestimated, dramatically for C05 (about 30% lower than experimental values). The precision of measured K_b and K_m is probably one of the main causes explaining the divergence between the model and experimental data. Indeed, using "best" or "medium" values of K_b and K_m can change quantitatively in a great extent the numerical values calculated by the model (Fig. 6). The hypothesis that the influence of saturation over Biot coefficient is linear-dependant is also a first approximation, and needs further experimental validation.

Finally, in the Fig. 7a (cement pastes) and b (mortars), a comparison of the predicted shrinkage is drawn between the present model and the model of [9], even if W/C ratios are higher in our present experiments, and that the model was only used for ordinary and high performance cement pastes. For M05, M08 and C08, the predicted shrinkage is slightly better with the proposed model. On the contrary, numerical values for C05 are better with the model of Baroghel-Bouny. The new model seems to globally improve the existing model. The other main advantage of the proposed model is to better take into consideration the difference in shrinkage for different W/C ratios, as for a given material type (cement paste or mortars).

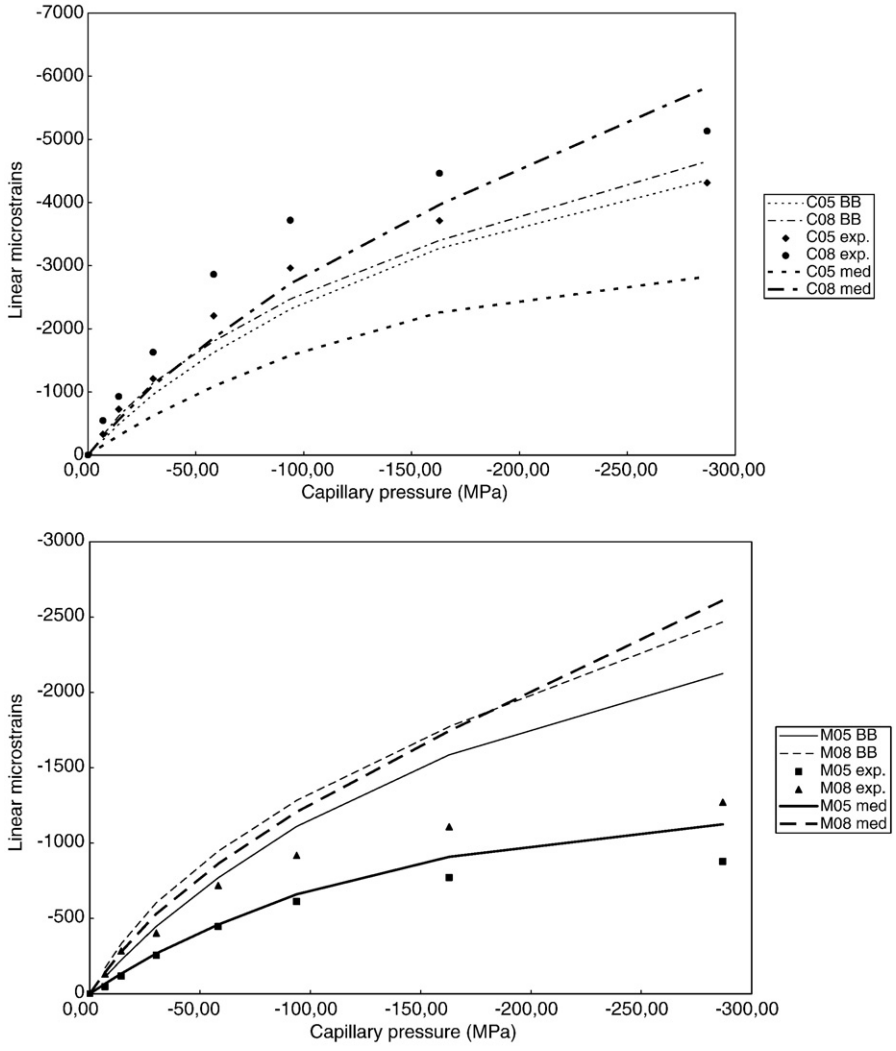

Fig. 7. a and b — Comparison between the proposed model (with medium values) and the model Baroghel-Bouny et al. for the shrinkage versus capillary pressure.

4. Conclusions

The present study has focused on studying, through water desorption curves, the hygrostructure and the desiccation shrinkage of both mortars and cement pastes. The aggregates appear to be quite independent from water desorption process, and do not strongly modify the hygrostructure of the cementitious matrix. Indeed, the shape of desorption curves or of porosity repartition for both cement pastes and mortars of a given W/C ratio is similar. The water desorption technique is of interest to study the beginning of the nanoporosity (pore diameters about 1 nm), which cannot be reached through mercury intrusion (pores larger than 6 nm in our present study). The influence of W/C ratio has also been observed on hygrostructure, showing that a higher one tends to shift the peaks of micro and sub-micro porosity to larger pores. The repartition of narrowest pores seems to be not affected by this ratio. The drying shrinkage was also studied through small step of desaturation, leading to almost free-structural shrinkage, thanks to smooth moisture gradients inside the samples. The shrinkage for the four tested materials is obtained, and the effects of aggregates or W/C ratio are well visible.

A simple model was also proposed to predict the shrinkage versus drying through some parameters which can all be determined experimentally by poromechanical experiments. Taking into consideration the effect of capillary pressure, and a linear evolution of matrix bulk modulus with saturation in a poromechanical approach tends to improve the model of Baroghel-Bouny for materials with a high W/C ratio, and can be also used for mortars. It can also be a good basis to an engineering model. Assessing an initial medium Biot coefficient for typical concrete (about 0.6) and a typical shape of water desorption curve [29], the model should be able through measure of the Young's modulus and Poisson's ratio to predict shrinkage versus relative humidity.

More poromechanical measurements, with other techniques (pore fluid changed to water or ethanol, tests on smoothly-dried specimen), could be performed to decrease the dispersion and improve the reliability of values used for the model, mainly for K_m. In addition, some experiences should be set up to determine the validity of the supposed linear evolution of K_m with saturation. This could be also achieved by a micromechanical approach of the problem, included porosity to solid matrix being a problem of, for instance, ellipsoidal vacuous inclusions into an elastic material.

References

[1] A. Carpinteri, P. Gambarova, G. Ferro, G. Plizzari, Fracture Mechanics of Concrete and Concrete Structures, Taylor & Francis Group, London, UK, 2007.
[2] G. Pijaudier-Cabot, B. Gérard, P. Acker, Creep, Shrinkage and Durability of Concrete and Concrete Structures, Hermes Science Pub., London, 2005.
[3] Z.P. Bažant, W.J. Raftshol, Effect of cracking in drying and shrinkage specimens, Cem. Concr. Res. 12 (1982) 209–226.
[4] V. Baroghel-Bouny, P.-C. Aïtcin, Shrinkage of Concrete, RILEM Publications, Paris, 2000.
[5] F.-J. Ulm, Z.P. Bažant, F.H. Wittmann, Creep, Shrinkage & Durability Mechanics of Concrete and other Quasi- Brittle Materials, Elsevier, New-York, 2001.
[6] I. Yurtdas, N. Burlion, F. Skoczylas, Triaxial mechanical behaviour of mortar: effects of drying, Cem. Concr. Res. 34 (2004) 1131–1143.
[7] Y. Bai, F. Darcy, P.A.M. Basheer, Strength and drying shrinkage properties of concrete containing furnace bottom ash as fine aggregate, Constr. Build. Mater. 19 (2005) 691–697.
[8] N. Burlion, F. Bourgeois, J.-F. Shao, Effect of desiccation on mechanical behaviour of concrete, Cem. Concr. Res. 27 (2005) 367–379.
[9] V. Baroghel-Bouny, M. Mainguy, T. Lassabatere, O. Coussy, Characterization and identification of equilibrium and transfer moisture properties for ordinary and high-performance cementitious materials, Cem. Concr. Res. 29 (1999) 1225–1238.
[10] V. Baroghel-Bouny, J. Godin, Experimental study on drying shrinkage of ordinary and high performance cementitious materials, in shrinkage of concrete, Proc. Of the Int. RILEM Workshop, RILEM Publications PRO 17, Paris, 2000, pp. 215–232.
[11] V. Baroghel-Bouny, Water vapour sorption experiments on hardened cementitious materials. Part I: essential tool for analysis of hygral behaviour and its relation to pore structure, Cem. Concr. Res. 37 (2007) 414–437.
[12] E.P. Barrett, L.G. Joyner, P.P. Halenda, The determination of pore volume and area distributions in porous substances. I— Computations from nitrogen isotherms, J. Amer. Chem. Soc. 73 (1951) 373–380.
[13] R. Vocka, C. Gallé, M. Dubois, P. Lovera, Mercury intrusion porosimetry and hierarchical structure of cement pastes. Theory and experiments, Cem. Concr. Res. 30 (2000) 521–527.
[14] S. Diamond, Mercury porosimetry, an inappropriate method for the measurement of pore size distributions in cement-based materials, Cem. Concr. Res. 30 (2000) 1517–1525.
[15] Acker P., Comportement mécanique du béton: apports de l'approche physico-chimique, PhD Thesis of Ecole Nationale des Ponts et Chaussées, Paris, Rapport de Recherche LPC 152, (in French), 1988.
[16] O. Coussy, P. Dangla, T. Labassatère, V. Baroghel-Bouny, The equivalent pore pressure and the swelling and shrinkage of cement-based materials, Mat. Struct. 37 (2004) 15–20.
[17] F.H. Wittmann, Deformation of concrete at variable moisture content, Mechanics of Geomaterials, John Wiley and Sons, 1985, pp. 425–459.
[18] Benboudjema F., Modélisation des déformations différées du béton sous sollicitations biaxiales. Application aux enceintes de confinement des bâtiments réacteurs des centrales nucléaires, Ph. D. Thesis, Université de Marne la Vallée, France, (in French), 2002.
[19] F.H. Wittmann, Surface tension; shrinkage and strength of hardened cement paste, Mat. Struct. 1 (1968) 547–552.
[20] Z.P. Bažant, J.-K. Kim, L. Panula, Improved prediction model for time dependant deformations of concrete: part 1—shrinkage, Mat. Struct. 24 (1991) 327–345.
[21] F. Bourgeois, N. Burlion, J.F. Shao, Modelling of elastoplastic damage in concrete due to desiccation shrinkage, Int. J. Numer. Anal. Methods Geomech. 26 (2002) 759–774.
[22] D. Chen, I. Yurtdas, N. Burlion, J.-F. Shao, Elastoplastic damage behaviour of a mortar subjected to compression and desiccation, J Eng Mech 133 (2007) 464–472.
[23] J.M. Torrenti, L. Granger, M. Diury, P. Genin, Modeling concrete shrinkage under variable ambient conditions, ACI Mater. J. 96 (1999) 35–39.
[24] O. Coussy, Poromechanics, John Wiley & Sons, New York, 2004.
[25] M. Lion, F. Skoczylas, B. Ledésert, Determination of the main hydraulic and poro-elastic properties of a limestone from Bourgogne (France), Int. J. of Rock Mech. And Min. Sci. 41 (2004) 915–925.
[26] F. Skoczylas, N. Burlion, I. Yurtdas, About drying effects and poro-mechanical behaviour of mortars, Cem. Con. Comp. 29 (2007) 383–390.
[27] N. Hearn, Effect of shrinkage and load-induced cracking on water permeability of concrete, ACI Material J. 96 (1999) 234–241.
[28] R.M. Espinosa, L. Franke, Inkbottle pore method: prediction of hygroscopic water content in hardened cement paste at variable climatic conditions, Cem. Concr. Res. 36 (2006) 1954–1968.
[29] M.T. Van Genuchten, A closed-form equation for predicting the hydraulic conductivity of unsaturated soils, Soil Sci. Soc. Am. J. 44 (1980) 892–898.